Bulletin of the JSME
Vol.20, No.1, 2025
Journal of Thermal Science and Technology

Analysis of Stirling engine's performance in recovering waste heat from wood pellet, coconut husk and bagasse

Nik Kechik Mujahidah NIK ABDUL RAHMAN*, Syamimi SAADON*, Abd Rahim ABU TALIB*, Ezanee GIRES*, Hanim SALLEH** and Nasser ABDELLATIF***

* Aerodynamics, Heat Transfer and Propulsion (AHTP) Group, Department of Aerospace Engineering, Faculty of Engineering, Universiti Putra Malaysia, Jalan Universiti 1, Serdang, Selangor 43400, Malaysia
E-mail: mimisaadon@upm.edu.my
** Department of Mechanical Engineering, College of Engineering, Universiti Tenaga Nasional (UNITEN), Putrajaya Campus, Jalan Kajang – Puchong, Kajang, Selangor 43000, Malaysia
*** Department of Electrical Engineering, Faculty of Engineering and Technology, Applied Science Private University, Al-Arab St. 21, Amman 11937, Jordan

Received: 3 November 2024; Revised: 17 January 2025; Accepted: 6 March 2025

Abstract
In recent years, industrial boilers that generate power from biomass have drawn a lot of attention. Nevertheless, a sizable portion of thermal energy is frequently lost to the environment as flue gas throughout the process. Stirling engine: a very efficient external combustion engine and little emissions as compared to other available engines, would be a good solution to overcome this issue as it can be used with any type of heat source. When the Stirling engine is connected to a heat source with a lower temperature, it exhibits a significant reduction in performance. Consequently, in this study a computational fluid dynamic (CFD) simulation model of Stirling engine was introduced in order to evaluate the possibility of recovering low temperature waste heat from biomass combustion. It has been shown to be effective in delivering useful, comprehensive information for further improvement of the engine. Then further parametric analysis will be investigated to enhance the engine's performance. The investigation involving waste heat from wood pellets, coconut husk and bagasse as heat source then demonstrates the engine's ability to recover and utilize heat as low as 70°C and generate power output ranging from 30 to 40 W and thermal efficiency of around 14%. Parametric analysis using different regenerator porosities, engine speeds and working fluid gases were also carried out to determine the optimal Stirling engine's performance. The results demonstrate optimum performance at 0.85-0.9 of porosity and engine speed of 700 rpm and above. Overall, the results showed promising outcomes of Stirling engine to recover low temperature heat from biomass.

Keywords : Biomass, Performance, Stirling engine, Waste heat recovery

1. Introduction

Over the past decades, the rising concern regarding global warming as well as the growing trend of increasing fuel prices has driven the world towards the task of improving the efficiency of their sites and reducing green-house gas emissions. More or less 168 million tons of biomass such as resources from coconut waste, sugar cane waste, palm oil waste, rice husks, municipal waste and forestry waste (Ozturk et al., 2017). Recent years have seen a considerable increase in interest in the use of biomass pellets for heating domestic water and the cofiring of coal and ground biomass for the production of electricity (Verma et al., 2009). The thermal efficiency range for the majority of industrial boilers is 60–90%. Nonetheless, the flue gas frequently releases a sizable portion of thermal energy into the surrounding air. As a result, heat has been lost, with exhaust flue gas being the main source. However, there is a large chance that the waste heat from industrial boiler flue gases can be recovered.

Stirling engine is an external combustion engine that operates in a closed cycle which means the fluid remains within the engine and continuously recycled (Gheith et al., 2018). Stirling engines, which are external combustion engines, are

Paper No.24-00388
[DOI: 10.1299/jtst.24-00388]

renowned for their great efficiency in comparison to steaming engines and their ability to employ nearly any heat source. If the Stirling engine is connected to a heat source that operates at a lower temperature, it exhibits a significant reduction in performance. Because of this, research is necessary to improve the Stirling engine's heat transfer efficiency when it is linked to a low-temperature heat source.

The Stirling engine's integration as a waste heat recovery system must take the heat transfer factor into account because it is an external combustion engine. The study also reveals that a lot of researchers employ artificial roughness, twisted tape or spiral devices, and vortex generators to increase the tubular heater's heat transfer factor (Maradiya et al., 2018). Powder can also be utilised as a heat carrier to improve heat transfer between the Stirling engine's heated storage (Zhang et al., 2016). One method of enhancing heat is to employ diffuser plates (Solomon and Qiu, 2018) and add conductivity material, such steel wool, to the engine heater (Song et al., 2015). Numerical modelling is frequently used prior to carrying out the experimental model approach, in addition to the experimental method which is extensively employed in simulating the optimal heat enhancement techniques in Stirling engines (Cheng and Chen, 2017). Studies about optimizing the heat transfer in the regenerator between the hot and cold side of the Stirling engine piston (Aksoy et al., 2015) also can be found widely in the literature.

The heat exchanger at the outer edge of the tubes should have a larger heating surface area than the walls of this hot vessel for large-power Stirling engines. The exterior side of the tubes, such as the exhaust waste gas side, exhibits the majority of the heat resistance during the heat transfer process in the Stirling engine heater (Saadon, 2019). In the existing Stirling engine technologies, much research has been devoted to enhancing heat transfer in the inner part of the tubular heater such as the regenerator, however the outer part of the tubular heater is also an important part of Stirling engine. The Stirling engine is an external combustion engine, meaning that all of the energy required to power the engine's movement comes from outside sources. As a result, losses resulting from heat bypass within the engine's structure or from heat transfer into and out of the engine may be more significant than mechanical losses (Hsieh et al., 2008). Even though it is generally acknowledged that the external area of a Stirling engine plays a crucial role in improving heat transmission for an external combustion engine, this aspect has not received much attention to date. The neglected optimization of the interface between heat source and heat engine gave rise to the failure of some approaches.

It is not a simple process to connect the biomass boiler and Stirling engine heater because this dictates the operating temperatures that may be obtained. As far as the authors were aware, the numerical models that were in use at lower temperatures were unstable and anticipated zero power output. We need to search for other engine configurations, like this one, in order to employ a Stirling engine for low potential heat. Additionally, based on literature reviews, Stirling engines with liquid pistons can run at extremely low temperatures but only produce a few watts of power, making thermoacoustic and free-piston engines less intriguing due to their higher prices and technological challenges.

Thus, this study will fill in the gap in order to decrease the heat transfer resistance and to enhance the heat transfer between the exhausted gas and the working medium, the geometries and heat transfer rate first will be simulated using Computational Fluid Dynamic (CFD). From the simulation, parameters such as engine speed, regenerator porosity and working fluid that affect the heat transfer rate will be identified. The new Stirling engine model tubular heater will then be tested after being integrated into the waste heat recovery system from biomass flue gas using the numerical technique.

2. Methodology

2.1 Modelling and geometry descriptions

Analysis of the Stirling engine for different geometries and addition of insulator materials will be carried out in ANSYS workbench R1 2020. The element modelling will be done using SOLIDWORKS and that model will be imported to ANSYS workbench including the meshing. At this state, thermal analysis to analyze the heat transfer rate will be carried out by determining temperatures and other thermal quantities that vary over time. The variation of temperature distribution over time is important to identify the most optimum design parameters for the improvement of heat transfer according to the research objectives. The numerical result will then be validated with the result of heat transfer of Stirling engine without biomass heat source and without the addition of thermal insulators conducted by the previous researcher. Figure 1 shows a schematic view of the Stirling engine and Tab. 1 depicts the dimensions of the Stirling engine's model.

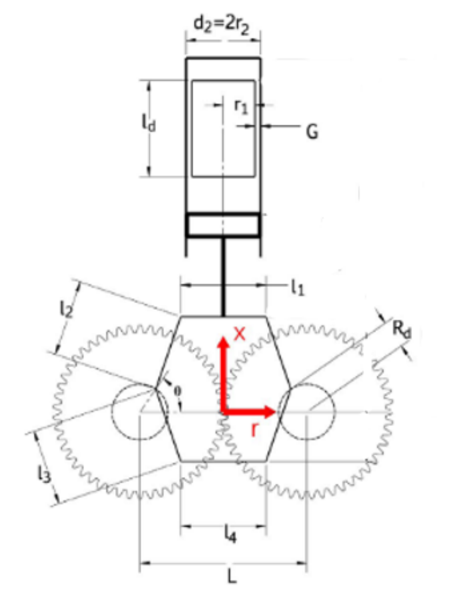

Fig. 1 Schematic view of the engine and nomenclature.

Table 1 Dimension of the numerical modelling of Stirling engine (Aksoy and Cinar, 2013).

Parameters	Dimensions
Working fluid	Air
r_1(mm)	42.25
r_2(mm)	43
l_d(mm)	155
l (mm) (for 1 to 4)	66
R_d(mm)	24.75
G (mm)	0.5
L (mm)	64

The displacer measures 84.5 mm in diameter and 155 mm in height, and it is situated 13.98 mm from the bottom surface. Most often, the narrow channel gap, G, is filled with regenerator materials, nevertheless, this model has no regenerator. This is according to the engine's baseline model by Ben-Mansour et al. (2017). As for the dead volume, its impact on power production and efficiency was examined by Gschwendtner and Bell (2017). It turns out that dead volume does not even participate in the heat transfer processes, which eventually leads to higher PV-work output, particularly at lower heat source temperatures. The energy model with the $k{-}\omega$ SST turbulence model was used for the analysis. The characteristics of the wall and its physical properties are reported in Table 2. The density was determined using the ideal gas model, while the heat capacity and viscosity were determined using kinetic theory. Ben-Mansour et al. (2017). evaluated the effect of viscous heating dissipation and the findings showed a slight variation, suggesting that this effect may not be significant. Additionally, tests revealed that the gravity effect had little effect on engine performance. As a result, neither gravity nor viscous heating effects were considered in this investigation. Since the pressure difference caused by gas flow inside the engine is just a tiny fraction of the total magnitude of pressure, the value of pressure is mainly determined by the ideal gas equation. Additionally, the Fourrier's law equation of conduction heat transport over exterior walls, is not included in the computational domain. Nonetheless, the programme was able to solve the conduction heat transfer without the need for computational geometry because the wall's thickness and features were specified in the wall boundary condition.

Three boundary conditions are defined to control movement of displacer and piston surface, where for top and bottom surface of displacer will move in the same movement in opposite motion compared to displacer surface motion. To ascertain how much the mesh density influences the simulation results, a mesh independence test is conducted. For this

[DOI: 10.1299/jtst.24-00388]

reason, the geometry model's mesh size is further optimized to create a large number of cells.

2.2 Mesh and time independence study

To make studying easier, the Stirling engine domain is split into four sub-domains (volumes). In accordance with Fig. 2, the volumes were given the names piston volume, engine gap volume, displacer top volume, and displacer bottom volume.

Table 2 Specification of the Stirling engine's model (Ben-Mansour et al., 2017).

Properties	Specifications
Engine rotation (rpm)	408
Cylinder's wall thickness (mm)	1
Cylinder's wall material	Steel
Cylinder's density (kg/m^3)	7840
Cylinder's wall thermal conductivity (W/m.K)	43
Cylinder's specific heat (J/kg.K)	450
Hot temperature (K)	800 K
Cold temperature (K)	300 K

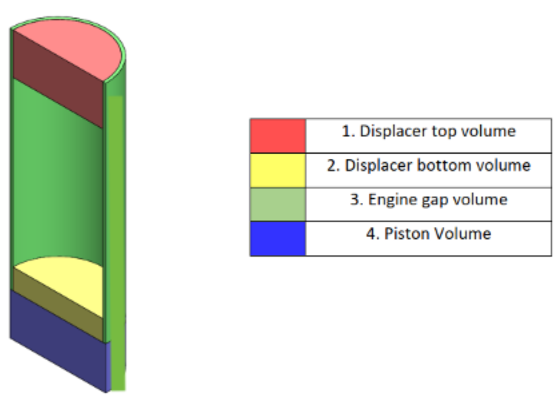

Fig. 2 The crosscut of the Stirling engine created four volumes.

In transient conditions, the user-defined function (UDF) and layered dynamic mesh function move the piston and displacer. The air acts as ideal gas, which is used as the working fluid. The heating surface's thermal boundary condition for the validation model is 775 K, whereas the piston surface's thermal boundary condition is 300 K. For this investigation, the basic pressure is 1 atm in the Stirling engine cycle. The Coupled Scheme Pressure-velocity Coupling technique was then used to discretize the equations since it exhibits a comparatively quick convergence compared to SIMPLE scheme. The flow equations' convergence threshold was set at 1.0×10^{-4}, while the energy equation was set at 1.0×10^{-8} .

[DOI: 10.1299/jtst.24-00388]

The overall mesh for this investigation is depicted in Fig. 3 (a), where the lowest and maximum cell sizes are 1.5 mm and 4 mm, respectively. The regenerator region, or gap between the displacer and engine, has a minimum cell size since it is so small and essential to use thick mesh there. The whole mesh was created using structured mesh, with a combination of quadrilateral 3D and hexahedral components. Mesh with an element size of 1.5 mm is shown in Fig. 3 (b) at the gap between the engine's wall and displacer. The temperature source for the hot surface (a) and the cold surface (b) under the boundary condition is depicted in Fig. 4. These hot and cold surfaces are different from the hot volume. Hot surface is the area where the cylinder's engine is exposed to the heat source temperature. Whereas hot volume or expansion volume, is the volume where the expansion process occurs due to the movement of the displacer and piston throughout the cycle. On the other side, the cold surface acts as a cooler with a temperature of 300 K, whereas cold volume or compression volume is the volume where the compression process occurs.

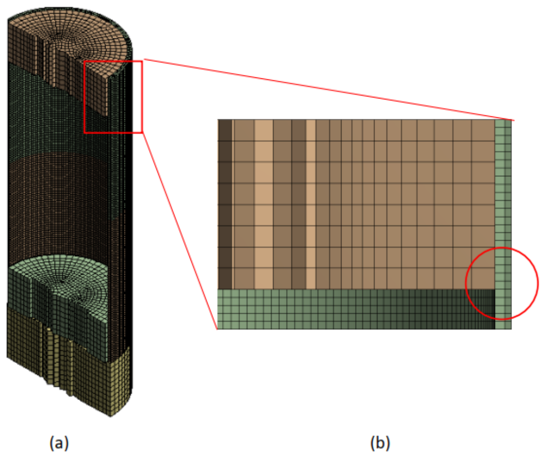

Fig. 3 Mesh created for this research (a) general mesh (b) finer mesh near the engine wall.

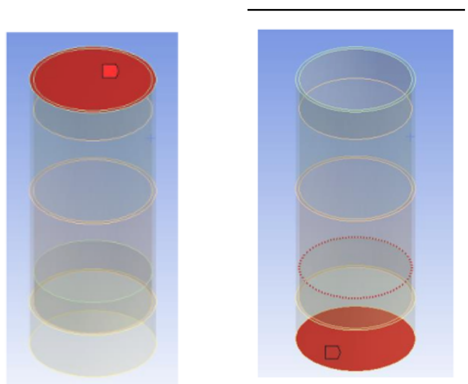

Fig. 4 A hot surface and a cold source surface are the two boundary conditions for a heat source.

To ascertain how much the mesh density influences the simulation results, a mesh independence test is conducted. For this reason, the geometry model's mesh size is further optimized to create a large number of cells. In other words, the geometry model's mesh count is raised further to ensure mesh independence. Because the models were complex and included of the air, heating, and cooling domains, tetrahedral unstructured grids were employed for the computational domain. For the area close to the fluid and regenerator walls, mesh enhancements were used. We examined four distinct mesh sizes. The grid dependency was verified for four different grid elements: 74,000, 78,000, 82,000, and 86,000. Dense mesh in the small space with intervals of two cells was one of the mesh types examined. Furthermore, 98 steps/cycle, or 1.25×10^{-3} s for time-step intervals, were used to examine each of these mesh sizes. For engine power and temperature,

[DOI: 10.1299/jtst.24-00388]

the variation, e(%), between the finest and coarsest grids is less than 0.1% and less than 4.21%, respectively. Consequently, the current work uses the grid settings from the later 86,000 grids for additional analysis.

2.3 Validation of the Stirling engine model

The outcomes of the Stirling engine validation are covered in this section. A previous study done by our team managed to validate the CFD model with real experimental data at 3.13% of discrepancy between the engine's power output (Kumaravelu et al., 2022). However, only a quarter of the Stirling engine was being modelled. Thus, in this paper, a more detailed CFD model will be created and simulated in order to precisely determine the performance of the engine.

The model is validated by comparing the simulation results obtained from this work with the experimental data obtained from Aksoy and Cinar (2013). The trend lines in Fig. 5 are drawn as a result of these findings. These CFD models and experimental data were used to establish the engine speed range of 380 to 545 rpm, with 300 K as the cold source temperature and 775 K as the hot source temperature.

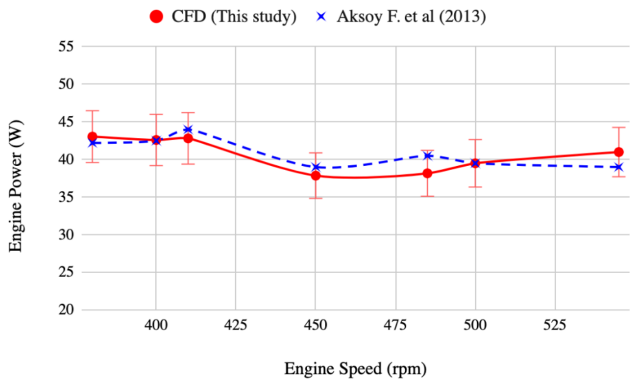

Fig. 5 Comparison of engine power obtained by numerical study and experiment conducted by Aksoy and Cinar (2013).

According to the CFD findings, when the engine is running at 500 rpm, there is the least variance of 0.02% and followed by engine speed at 400 rpm with slight variance at 0.23%. On the other hand, while the engine is running at 485 rpm, the biggest variance is 5.77% and followed by engine speed at 545 rpm with 5.10%. Thus, the engine's model can be considered for further analysis as the percentage error is only 6% and below. An acceptable average difference of 2.68% was found when comparing the trend lines of the experimental and CFD data for each engine speed that was used. This goes to show that even if the preliminary comparison result indicates a slight divergence, it may still be used to estimate an engine's power output. The findings show that choosing the right engine speed for the CFD model to achieve the least amount of variance from the actual experimental value is a crucial parameter in this study.

Additionally, the current results' inaccuracy can be also attributed to the unconsidered effects of heat conduction loss through material thickness and flow leakage from the cylinder to buffer space through the piston rings. Additionally, it is anticipated that using a more appropriate turbulence model during simulation will result in an additional change in accuracy. Therefore, in our study standard wall functions for the k-omega turbulence model were used, which is one of the most popular models for simulating the impact of turbulent flow conditions. In the boundary layer area along the wall, this turbulence model performs well in terms of accuracy. Thus, the chosen model satisfies the requirements for accuracy and dependability in the fluid flow and heat transfer analysis under study.

The displacer moves downward at the beginning of the cycle, forcing the air in the cylinder to travel to the engine's hot end. The power piston is pushed outward and towards the crankshaft as a result of the air heating up and expanding. The air travels to the cold side of the cylinder as the displacer rises. The power piston is drawn inward and away from the crankshaft as the air cools and constricts.

3. Results and discussion

To determine whether this type of Stirling engine can recover heat from a low-grade temperature, an experimental test rig was set up to recuperate waste heat from biomass as in Fig. 6. 1 kg of biomass was burned in a combustion chamber and the waste heat resulting from this burning process was channeled through a pipe to a steel wall that acts as the cylinder wall of Stirling engine. A heat flux sensor of sensitivity 0.26×10^{-6} V/(W.m^2) was used in this set up. Four pieces of type-K thermocouple were utilized in this experiment. Three of them were connected to the inner part of the combustion chamber at three different heights to measure the average temperature of the combustion heat inside the chamber, which would be the temperature of the exhaust gas and the heat source. Another thermocouple is attached to the engine wall along with the heat flux sensor. This would be the wall temperature. These thermocouples and heat flux sensors were connected to the data logger to measure the temperature and voltage of the exhaust heat.

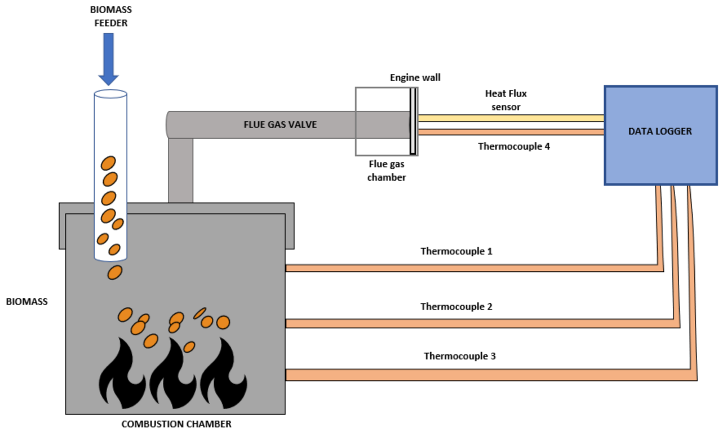

Fig. 6 Experimental setup for recuperation of waste from biomass.

During the combustion process, three types of biomass; wood pellet, coconut husk and bagasse were inserted into the combustion chamber through the biomass feeder 1kg at a time. A combustion basket was placed in the combustion chamber to make sure the biomass combusted evenly with the butane gas applied under the combustion chamber. The results of temperature calibration are shown in Fig. 7. From the temperature calibration graph, it is clearly shown that the temperature ranges from 60 to 70°C.

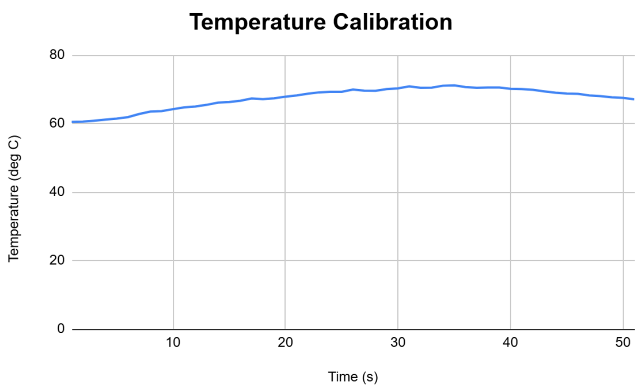

Fig. 7 Temperature calibration test results.

From the experiment, the voltage is measured using the heat flux sensor, then eventually the heat flux will be calculated using Eq. (1). The heat transfer coefficient is then calculated using Eq. (2). This means that the heat transfer coefficient will be determined experimentally. From this experimental testing, for a 1 kg of wood pellet as biomass source, a heat flux of 402.60 W/m^2 was found, with a temperature heat source of only 339.9 K and a difference of temperature between the waste heat and the wall at the hot side of 6.6 K. This results in a heat transfer coefficient of 60.74 W/$m^2.K$ calculated for this beta-type of Stirling engine. With these findings from the experiment, a simulation was run using the Stirling engine's CFD model validation previously. Taking into consideration the validation results from the previous section, the following descriptions and results will depict the simulation done at 400 rpm of speed. This engine speed is used as it shows the lowest error discrepancy in previous validation. From these numbers, it is evident that the gas close to the cylinder side wall enters the hot zone at around 300 K, whereas the gas close to the displacer side wall exits the narrow channel at about 280 K.

$$\emptyset = \frac{V}{Heat\ flux\ sensitivity} \quad (1)$$

with $\emptyset$ is the heat flux for each biomass waste heat in W/m^2 and V is the voltage.

$$h = \frac{\emptyset}{\Delta T} \quad (2)$$

where h is the heat transfer coefficient in W/(m^2.K) and ΔT is the difference of temperature between the heat source coming out from the chamber and the wall temperature.

Experiments were also run for another two types of biomasses which are coconut husk and bagasse. The experimental set up for both was the same as previously. For a 1 kg of coconut husk and bagasse each, a heat flux of 243.18 W/m^2 and 569.91 W/m^2 were found respectively. This corresponds to a temperature heat source of only 335.3 K for coconut husk and 334.5 K and a difference of temperature between the waste heat and the wall at the hot side of 11.3 K and 10.2 K respectively. This leads to a heat transfer coefficient of 21.62 W/(m^2.K) and 55.71 W/(m^2.K).

Next, this value of heat transfer coefficient and heat flux from biomass will be inserted in the CFD model to simulate the performance of the Stirling engine. The results of power and engine speed relationship are presented in this section. Figure 8 below tabulate the total engine power produced with these three biomasses as heat sources and a comparison with previous studies done by Ben-Mansour et al. (2017) using CFD modelling and by Aksoy and Cinar (2013) experimentally, but with different heat sources, were shown in order to verify that the results from our simulations are acceptable and within the same ranges. As shown in Fig. 8, it can be seen that all the three biomasses generate a more or less equal amount of power output. The engine power produced by using wood pellets as heat source ranging from 16 to 39 W, with highest value at engine speed of 410 rpm. This is rather similar for bagasse as well, since the power generated from bagasse varies from 17 to 39 W, with peak value occurring also during 410 rpm of engine speed. As for coconut husk, it goes from 21 to 41 W and peaks at the same amount of engine speed. These results prove that this type of engine could possibly recover waste heat from as low as 60 to 70°C and still be able to produce a reasonable amount of power output.

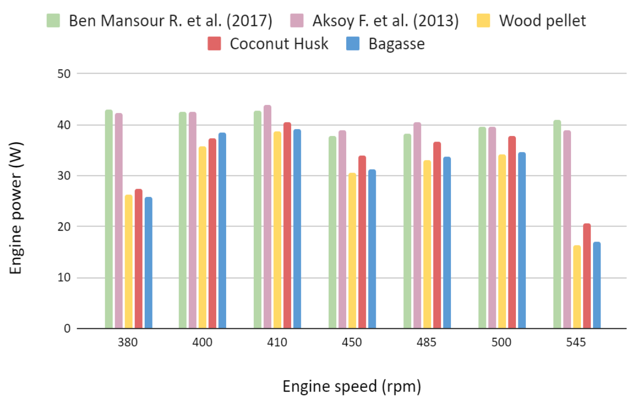

Fig. 8 Comparison between engine power with biomass waste as heat source with previous studies by Aksoy and Cinar (2013) and Ben-Mansour et al. (2017).

[DOI: 10.1299/jtst.24-00388]

All biomasses show similar trendlines with previous study in which the optimal power output of the engine happens at 400 to 410 rpm which can reach around 40 W. The power output of the engine shows degradation after engine speed 500 rpm. This is somehow aligned with previous studies by Aksoy and Cinar (2013) and Ben-Mansour et al. (2017) where power output starts to decrease a bit at this level of engine speed. Increased heat resistance, vibration of the engine, friction between moving parts, shuttle losses and pumping losses, the flow resistance of the working gas and other factors are likely to cause mechanical loss at higher rotational speeds. The leakage of working gas from the side clearance of the piston and the displacer might be also important loss, which varies with rotational speed. Therefore, for further parametric analysis, this study will try to focus more on the engine's performance results at 400 to 500 rpm of engine speed.

Using biomass as a heat source, the Stirling engine operates at low temperatures compared to the previous experiment. Therefore, the power output typically decreases as the engine speed increases due to several reasons that can be considered. At low temperatures of biomass waste heat, there may be limitations in movement of heat between the cold and hot reservoirs which lead to an incomplete heat transfer cycle. Increasing the engine speed doesn't necessarily improve heat transfer efficiency, which means the engine cannot effectively utilize the available temperature differential to produce work.

There are also possibilities of an increase in mechanical loss. This is caused by low temperature exacerbating mechanical losses within the engine, such as frictional losses in displacer, piston, and other moving parts. As the engine speed increases, these losses become bigger and reduce the net power output. With low temperatures of biomass heat source, the viscosity of the working fluid may increase, leading to higher internal resistance within the engine. This increased resistance requires more energy to overcome, resulting in lower efficiency and reduced power output.

Additionally, the engine efficiency with all the three-biomass waste as heat sources were also calculated and depicted in Fig. 9. The model predicts an average of 12 to 14% engine efficiency, which seems in coherence with a study done by Garcia et al. (2022) that also used wood pellets as heat source.

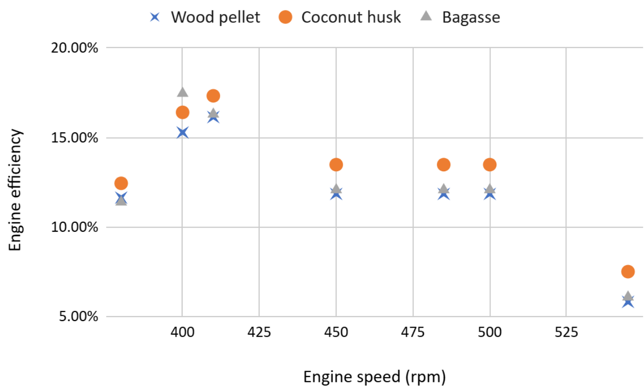

Fig. 9 Thermal efficiency of the engine for different biomass waste heat sources.

For a rotation speed of 410 rpm, the engine was able to produce an estimation of power output of 38.77 W and thermal efficiency of 16.14%. Meanwhile, for a higher speed at 545 rpm, the work done is slightly higher at 16.36 W with quite low thermal efficiency at 5.82%. The result shows that the engine efficiency drops when it reaches 545 rpm engine speed and above.

The decrease in efficiency of the engine as engine speed increases is caused by the increasing frictional losses in the engine. Higher engine speeds lead to faster movement of displacer, pistons and other moving parts. The increased frictional forces lead to thermal energy dissipation resulting in reduced power output. Furthermore, with faster operation by the faster engine speed, the time available for heat transfer between the working fluid and the hot and cold sources decreases which leads to incomplete heating and incomplete cooling. Incomplete heating is a condition where the working fluid may not reach the full desired temperature at the hot volume, decreasing the thermal energy input to the cycle. Incomplete cooling, as contrast, the working fluid may not fully discharge heat at the cold volume, abandoning some thermal energy unused.

At higher speeds, the engine does not have enough time for heating and cooling, similarly there may not be enough time for complete compression and expansion of the working fluid within the cylinders which can be considered as

[DOI: 10.1299/jtst.24-00388]

incomplete expansion and compression. This can lead to lower efficiency as the engine fails to extract maximum work from the available heat input.

Additionally, phenomena of efficiency degrading are also probably caused by the increase in internal heat generation. It is because higher speeds often result in higher internal pressures within the engine. Increased compression leads to more internal friction, resulting in additional thermal energy generation within the engine cycle. This excess heat contributes to energy losses and diminishes overall efficiency. From the result, it can be concluded that the optimal engine speed where the power output is maximized while the efficiency is still acceptable is while the engine runs between 400 and 410 rpm.

The effects of the regenerator porosity on engine power output at rotational speed of 400 rpm were calculated and shown in Fig. 10. The result shows the highest work done for the Stirling engine using wood pellet as the biomass heat source is with regenerator porosity 0.9. While for the coconut husk and bagasse shows the highest work done obtained when the regenerator porosity is 0.85. From the result, it can be concluded that the optimal porosity value for the engine regenerator where the power output is maximized is when the porosity is at 0.9 for wood pellet, and 0.85 for coconut husk and bagasse.

When the regenerator porosity is around 0.9 (or 90%), it means that 90% of the volume is occupied by voids or passages for the working fluid to flow through. This high porosity allows for effective heat transfer between the working fluid and the solid matrix of the regenerator. Higher porosity typically means more surface area for heat transfer between the working fluid and the regenerator matrix. This promotes efficient heat exchange, which is crucial for the performance of the engine. However, increasing porosity also increases the pressure drop through the regenerator. This can reduce the engine's efficiency if the pressure drop becomes too high, as it would require more energy to overcome. This is the reason why the engine power is optimal at porosity 0.85 to 0.9 but degrading approaching 1.0. The previous researcher mentioned that a porosity of around 0.9 is often found to be a good compromise, as it allows for sufficient heat transfer while keeping pressure drops within acceptable limits.

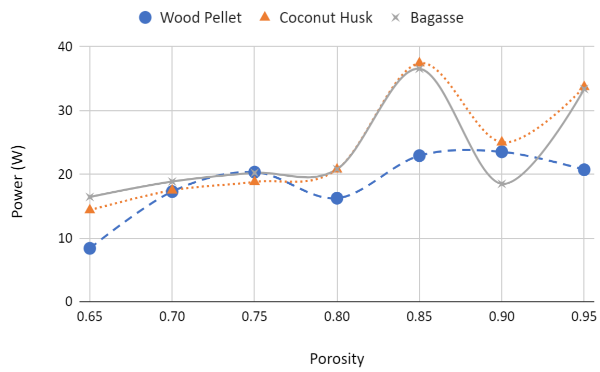

Fig. 10 Power output with different porosity of the engine at 400 rpm.

The effects of different rotational speeds on engine power output with optimized porosity level (0.9 for wood pellet and 0.85 for coconut husk and bagasse) are shown in Fig. 11 for every type of biomass heat source. The trendlines show a similar pattern for all biomass as the engine power keeps increasing while the speed is raised from 600 rpm to 1200 rpm.

The effects of using different gas as working fluid on engine power output with optimized porosity level and engine speeds for wood pellet, coconut husk and bagasse, are shown in Fig. 12 for every type of biomass heat source. The different gas used were helium, hydrogen and nitrogen. The bar chart shows a similar pattern for all biomass as the helium gas predicts highest engine power, followed by nitrogen and hydrogen. This could be due to the thermal conductivity level of these gas. Because these gases have a higher thermal conductivity than air, more heat is likely to be dissipated from the cylinder-side wall by convective heat transfer, which could explain the modest decrease in power production. the differences in thermal properties, hydrogen, helium, and nitrogen have different characteristics because the amount of leakage from the piston side clearance also varies. Additionally, the friction coefficient also changes, which significantly affects further mechanical losses compared to when using air as working fluid.

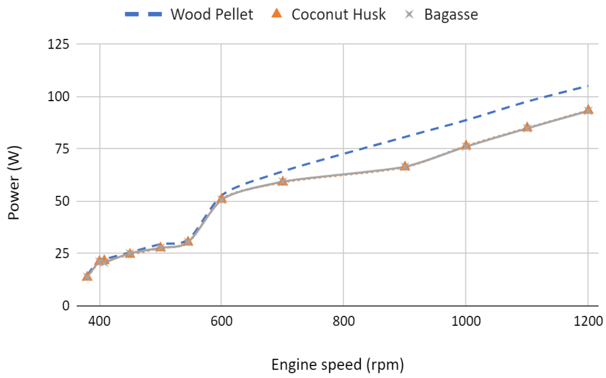

Fig. 11 Power output with different engine speed.

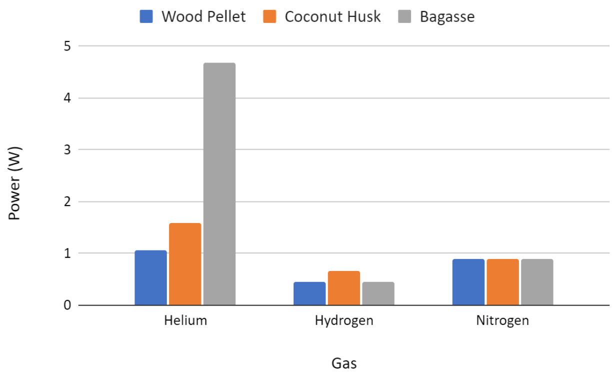

Fig. 12 Power output and work done with different working fluid gas for all biomass at 408 rpm.

4. Conclusion

Experimental and simulation data were acquired to assess heat transfer performance in a beta-type Stirling engine, designed for potential adaptation in biomass applications. This study carries out simulations on 3D CFD model of Stirling engine to examine the engine's performance when paired with a low-temperature biomass source. The model facilitates analysis of operational parameters challenging to measure directly, enabling estimation of performance under varied conditions beyond the validation study. Notably, the temperature distribution across the heater wall appears appropriate. The primary objective of this investigation, which is to assess the feasibility of utilizing a low-temperature heat source for power generation with this engine type, is effectively achieved. Results indicate a satisfactory power output compared to reference studies, suggesting potential utilization of this engine for power generation from heat sources as low as 60°C. These findings hold a promising future for research on Stirling engine with low-temperature heat sources.

The engine was able to produce an estimated power output of 38.77 W, 40.49 W and 39.06 W with the waste heat from wood pellet, coconut husk and bagasse respectively as external heat source at 410 rpm of engine speed. Additionally, the thermal efficiency at this point is around 16 to 17% for all the three biomass heat sources. Nonetheless, some drawbacks were noticed at higher engine speed, where the power output produced starts to decrease, likely due to mechanical loss at this speed.

Replacing air with He, H_2 and N_2 as working fluid gas, gives an impact to the power output and thermal efficiency of the engine. When compared to air, these gases have a higher thermal conductivity level, which causes more heat to be dissipated from the cylinder-side wall by convection heat transfer. This could explain the modest decrease in power production. Nonetheless, by focusing on the thermal behavior, the temperature level of the hot and cold volume of these three gasses is higher compared to the one by using air as working fluid.

[DOI: 10.1299/jtst.24-00388]

Acknowledgments and conflicts of interest

This research was funded by a matching grant (Matching Grant: UPM-JORDAN/2022/9300487) from Universiti Putra Malaysia.

References

Aksoy, F. and Cinar, C., Thermodynamic analysis of a beta-type Stirling engine with rhombic drive mechanism. Energy Conversion and Management, Vol. 75, (2013), pp. 319-324.

Aksoy, F., Karabulut, H., Cinar, C., Solmaz, H., Ozgoren, Y.O. and Aysal, F.E., The Thermodynamic Analysis of a Beta Type Rhombic Drive Stirling Engine. 1st International Conference on Environmental Science and Technology (2015).

Ben-Mansour, R., Abuelyamen, A. and Mokheimer, E. M. A., CFD analysis of radiation impact on Stirling engine performance. Energy Conversion and Management, Vol. 152, (2017), pp. 354-365.

Cheng, C. H. and Chen, Y. F., Numerical simulation of thermal and flow fields inside a 1-kW beta-type Stirling engine. Applied Thermal Engineering, Vol. 121, (2017), pp. 554-561.

García, D., Suárez, M.-J., Blanco, E. and Prieto, J.-I., Experimental and Numerical Characterisation of a Non-Tubular Stirling Engine Heater for Biomass Applications. Sustainability, Vol. 14, (2022), 16488. DOI: 10.3390/su142416488

Gheith, R., Hachem, H., Aloui, F. and Ben Nasrallah, S., Stirling Engines. Comprehensive Energy Systems Energy conversion, Vol. 4, (2018), pp.169-208.

Gschwendtner, M. and Bell, G., The myth about dead volume in Stirling engines. Proceedings of the Institution of Mechanical Engineers, Part C: Journal of Mechanical Engineering Science, Vol. 231, No. 19, (2017), pp. 3665-3675.

Hsieh, Y. C., Hsu, TC. and Chiou, JS., Integration of a free-piston Stirling engine and a moving grate incinerator, Vol. 33, (2008), pp. 48-54.

Kumaravelu, T., Saadon, S. and Abu Talib, AR., Heat transfer enhancement of a Stirling engine by using fins attachment in an energy recovery system. Energy, Vol. 239, (2022), 121881. DOI: 10.1016/j.energy.2021.121881

Maradiya, C., Vadher, J. and Agarwal, R., The heat transfer enhancement techniques and their Thermal Performance Factor. Beni-Suef University Journal of Basic and Applied Sciences, Vol. 7, No. 1, (2018), pp. 1-21.

Ozturk, M., Saba, N., Altay, V., Iqbal, R., Hakeem, K. R., Jawaid, M. and Ibrahim, F. H., Biomass and bioenergy : An overview of the development potential in. Renewable and Sustainable Energy Reviews, Vol. 79, (2017), pp. 1285-1302.

Saadon, S., Possibility of Using Stirling Engine as Waste Heat Recovery - Preliminary Concept. IOP Conference Series: Earth and Environmental Science, Vol. 268, No. 1, (2019), 012095. DOI: 10.1088/1755-1315/268/1/012095

Solomon, L. and Qiu, S. Computational Analysis of External Heat Transfer for a Tubular Stirling Convertor. Applied Thermal Engineering, Vol. 13, No. 7, (2018), pp. 138-141.

Song, Z., Chen, J. and Yang, L., Heat transfer enhancement in tubular heater of Stirling engine for waste heat recovery from fl ue gas using steel wool. Applied Thermal Engineering, Vol. 87, (2015), pp. 499-504.

Verma, V. K., Bram, S. and Ruyck, J. De., Small scale biomass heating systems : Standards , quality labelling and market driving factors – An EU outlook. Biomass and Bioenergy, Vol. 33, No. 10, (2009), pp. 1393-1402.

Zhang, H., Gowing, T., Degrève, J., Leadbeater, T. and Baeyens, J., Use of Particle Heat Carriers in the Stirling Engine Concept. Energy Technology, Vol. 4, No. 3, (2016), pp. 401-408.